Luminescent *nido*-Carborane–Diphosphine Anions [(PR2)2C2B9H10]− (R = Ph, iPr). Modification of Their Luminescence Properties upon Formation of Three-Coordinate Gold(I) Complexes

Olga Crespo,[†,‡] Mª. Concepción Gimeno,[†] Peter G. Jones,[§] Antonio Laguna,*[,†] José Mª. López-de-Luzuriaga,[||] Miguel Monge,[||] Juan L. Pérez,[‡] and Miguel A. Ramón[‡]

Departamento de Química Inorgánica, Instituto de Ciencia de Materiales de Aragón, Universidad de Zaragoza-CSIC, 50009 Zaragoza, Spain, Institut für Anorganische und Analytische Chemie der Technischen Universität, Postfach 3329, D-38023 Braunschweig, Germany, Departamento de Química, Universidad de la Rioja, Grupo de Síntesis Química de La Rioja UA-CSIC, Madre de Dios 51, 26006 Logroño, Spain, and Escuela Politécnica Superior de Huesca. Carretera de Cuarte s/n. 22071 Huesca, Spain

The free *nido*-diphosphine anions [(PR2)2C2B9H10]− (R = Ph, iPr) show luminescence properties whereas the *closo*-diphosphines [(PR2)2C2B10H10] do not. Four families of three-coordinate complexes of stoichiometry [Au{(PR2)2C2B10H10}L]OTf (L = tertiary phosphine) and [Au{(PR2)2C2B9H10}L] have been studied in order to analyze the influence of the *closo*- or *nido*-nature of the diphosphine, the monophosphine coordinated to gold and the substituent at the diphosphine on the luminescence of the complexes. Only the *nido*-derivatives show luminescence. The maxima of the emissions are shifted to lower energies than those of the corresponding free *nido*-diphosphines. When the substituent at the diphosphine is phenyl, a new emission appears, which has been assigned as arising from a metal to ligand charge transfer [Au→π*(L)] excited state.

Introduction

The synthesis and properties of dicarba-*closo*-dodeca-boranes were first reported at the end of 1963, and Wies-boeck and Hawthorne showed in 1964 that the *ortho*-carborane [1,2-C2B10H12] could be partially degraded[1] to afford the corresponding *nido*-species [7,8-C2B9H12]−. Since then, both *closo*- and *nido*-carboranes have proved to be excellent bulky and stable building blocks that allow the synthesis of a wide range of molecules.[2] Such carboranes have recently been shown to have a variety of applications in material science (display devices[3], nonlinear optical materials,[4] recognition systems,[5] special polymers[6]), catalysis (olefin polymerization[7]), or medicine (BNCT[8]) which make carborane chemistry an interesting growth area. As a part of

our studies on carborane chemistry, we have recently reported the luminescence properties of tetranuclear gold clusters of stoichiometry [Au4{(PR2)2C2B9H10}2L2] (L = AsPh3 or PR3).[9] In these complexes, two of the gold atoms were formally assigned oxidation state +1, and the other two zero; we proposed that the Au (+1) centers were responsible for the

* To whom correspondence should be addressed. E-mail: alaguna@posta.unizar.es. Phone: + 34-976-761185. Fax: + 34-976-761187.
† Universidad de Zaragoza-CSIC.
‡ Escuela Politécnica Superior de Huesca.
§ Institut für Anorganische und Analytische Chemie der Technischen Universität.
|| Universidad de la Rioja.

(1) Wiesboeck, R. A.; Hawthorne, M. F. *J. Am. Chem. Soc.* **1964**, *86*, 1642.
(2) Bregadze, V. I. *Chem. Rev.* **1992**, *92*, 209.

(3) (a) Lee, S.; Mazurowski, J.; Ramseyer, G.; Dowben, P. A. *J. Appl. Phys.* **1992**, *72*, 4925. (b) Byun, D. G.; Hwang, S. D.; Eowben, P. A.; Perkin, F. K.; Filips, F.; Ianno, N. J. *J. Phys. Lett.* **1994**, *64*, 1968. (c) Hwang, S. D.; Byun, D. G.; Ianno, N. J.; Dowben, P. A.; Kim, H. R. *Appl. Phys. Lett.* **1996**, *68*, 1495. (d) Perkins, R. K.; Rosenberg, R. A.; Lee, S. W.; Dowben, P. A. *J. Appl. Phys.* **1991**, *69*, 4103.
(4) (a) Base, K.; Tierney, M. T.; Fort, A.; Muller, J.; Grinstaff, M. W. *Inorg. Chem.* **1999**, *38*, 287. (b) Frendich, W.; Harvey, J. E.; Kaszynsky, P. *Inorg. Chem.* **1999**, *38*, 408.
(5) (a) Baadr, I. H. A.; Diaz, M.; Hawthorne, M. F.; Bachas, L. G. *Anal. Chem.* **1999**, *71*, 1371. (b) Hawthorne, M. F.; Zheng, Z. *Acc. Chem. Res.* **1997**, *30*, 267.
(6) (a) Douglas, A. G.; Czuprynski, K.; Mierzwa, M.; Kaszynski, P. *J. Mater. Chem.* **1998**, *8*, 2391. (b) Douglas, A. G.; Czuprynski, K.; Mierzwa, M.; Kaszynski, P. *Chem. Mater.* **1998**, *10*, 2399.
(7) (a) Crowther, D. J.; Swenson, D. C.; Jordan, R. F. *J. Am. Chem. Soc.* **1995**, *117*, 10403. (b) Bowen, D. E.; Jordan, R. F. *Organometallics* **1995**, *14*, 3630.
(8) Soloway, A. H.; Tjarks, W.; Barnum, A.; Rong, F.-G.; Barth, R. F.; Codogni, I. M.; Wilson, J. G. *Chem. Rev.* **1998**, *98*, 1515.
(9) Calhorda, M. J.; Crespo, O.; Gimeno, M. C.; Jones, P. G.; Laguna, A.; López de Luzuriaga, J. M.; Pérez, J. L.; Ramón, M. A.; Veiros, L. F. *Inorg. Chem.* **2000**, *39*, 4280.
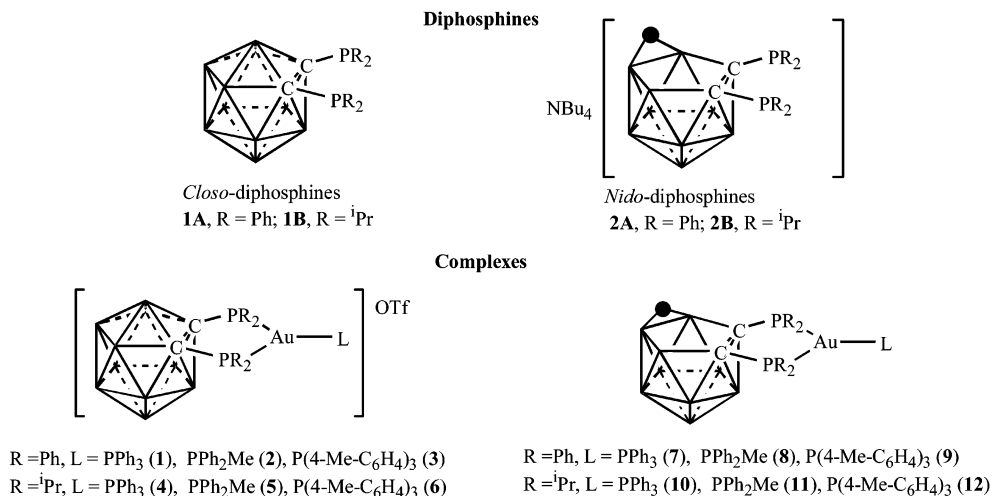
Diphosphines

Closo-diphosphines
1A, R = Ph; **1B**, R = ^{i}Pr

Nido-diphosphines
2A, R = Ph; **2B**, R = ^{i}Pr

Complexes

R =Ph, L = PPh$_3$ (**1**), PPh$_2$Me (**2**), P(4-Me-C$_6$H$_4$)$_3$ (**3**)
R = ^{i}Pr, L = PPh$_3$ (**4**), PPh$_2$Me (**5**), P(4-Me-C$_6$H$_4$)$_3$ (**6**)

R =Ph, L = PPh$_3$ (**7**), PPh$_2$Me (**8**), P(4-Me-C$_6$H$_4$)$_3$ (**9**)
R = ^{i}Pr, L = PPh$_3$ (**10**), PPh$_2$Me (**11**), P(4-Me-C$_6$H$_4$)$_3$ (**12**)

Figure 1. Ligands and complexes studied.

observed light emission. This result supports the view that, in the case of gold clusters, the d^{10} gold(I) centers, which are only a short distance from each other, are the centers responsible for the luminescence.[10] Nevertheless, in addition to the gold(I)−gold(I) bonding interaction, the role of the environment around these centers cannot be neglected; thus, recent reports by Che and co-workers address the gold−ligand bonding as the salient factor affecting the photoluminescence of gold(I) complexes.[11,12] As far as we know, these complexes, and the recently reported[13] [Hf(η^5:η^1-CpCMe$_2$CB$_{10}$H$_{10}$C)$_2$] which shows photo-, electro-, and mechanoluminescence, are the only luminescent *ortho*-carborane derivatives containing transition metals.

Three-coordinate gold(I) complexes have also been shown to exhibit luminescence.[14−21] Che et al.[22] have recently analyzed the role of gold−gold interactions in such homoleptic three-coordinate systems. In the present extension of our studies of carborane chemistry,[23] we analyze the luminescence behavior of complexes (Figure 1) of stoichiometry [Au{(PR$_2$)$_2$C$_2$B$_{10}$H$_{10}$}L]OTf and [Au{(PR$_2$)$_2$C$_2$B$_9$H$_{10}$}L] (OTf = CF$_3$SO$_3$; L = tertiary phosphine; R = Ph, ^{i}Pr) and evaluate

Table 1. Excitation and Emission Spectra for the *nido*-Diphosphines and *nido*-Complexes

compd	ex (nm)	em (nm) solid RT	em (nm) solid 77 K	em (nm)^b (CH$_3$)$_2$CO
NBu$_4$(dppnc) (**2A**)	332	482	465	429 (379)
[Au(dppnc)(PPh$_3$)] (**7**)	332	540	529	528 (338)
	460	670	676	603 (453)
[Au(dppnc)(PPh$_2$Me)] (**8**)	335	521	513	530 (338)
	412	640	653	576 (423)
[Au(dppnc){P(4-MeC$_6$H$_4$)$_3$}] (**9**)	337	513	506	534 (396)^c
	459	614	633	
NBu$_4$(dipnc) (**2B**)	335	484	488	422 (340)
[Au(dipnc)(PPh$_3$)] (**10**)	337	508	507	514 (331)
[Au(dipnc)(PPh$_2$Me)] (**11**)	327	512	505	512 (338)
[Au(dipnc){P(4-MeC$_6$H$_4$)$_3$}] (**12**)	322	508	503	512 (336)

^{a} dppnc = [(PPh$_2$)$_2$C$_2$B$_9$H$_{10}$]$^-$, dipnc = [(P^{i}Pr$_2$)$_2$C$_2$B$_9$H$_{10}$]$^-$. ^{b} Excitation energy in brackets, concentration 2 × 10^{-3} M. ^{c} Broad.

the influence of the neutral monophosphine ligand, the substituents on the diphosphine ligand, and the partial degradation of the carborane cage on the emission properties of these complexes.

Results and Discussion

Photophysical Studies. Free Diphosphines. Both *nido*-diphosphines (**2A,B**) show similar excitation and emission profiles in the solid state and in solution, while the neutral carboranes (**1A,B**) are not luminescent. Excitation at 332 (diphenyl) or 335 nm (diisopropyl) leads to emissions at 482 and 484 nm in the solid state or 429 (excitation at 379) and 422 nm (excitation at 340) in solution, respectively (Table 1). The luminescence of the *nido*-carborane derivatives is probably related to a significant change of the electronic structure in the carborane produced when the starting material (*closo*) loses one boron atom in a nucleophilic attack to give rise the anionic *nido*-diphosphine. The maxima of emission and excitation are very similar for **2A** (R = Ph) and **2B** (R = ^{i}Pr). Greater differences in the energy values would be expected if the substituents at phosphorus centers played an

(10) Forward, J. M.; Fackler, J. P., Jr.; Assefa, Z. In *Optoelectronic Properties of Inorganic Compounds*; Roundhill, D. M., Fackler, J. P., Jr., Eds; Plenum Press: New York, 1999; p 195.
(11) (a) Fu, W. F.; Chan, K. C.; Miskowsky, V. M.; Che, C. M. *Angew. Chem., Int. Ed.* **1999**, *38*, 2783. (b) Fu, W. F.; Chan, K. C.; Cheung, K. K.; Che, C. M. *Chem. Eur. J.* **2001**, *7*, 4656.
(12) Leung, K. H.; Phillips, D. L.; Tse, M. C.; Che, C. M.; Miskowsky. V. M. *J. Am. Chem. Soc.* **1999**, *121*, 4799.
(13) Hong, E.; Jang, H.; Kim, Y.; Jeoung, S. C.; Do, Y. *Adv. Mater.* **2001**, *13*, 1094.
(14) McCleskey, T. M.; Gray, H. B. *Inorg. Chem.* **1992**, *31*, 1734.
(15) Che, C. M.; Yip, H. K.; Yam, V. W. W.; Cheung, P. Y.; Lai, T. F.; Shieh, S. J.; Peng, S. M. *J. Chem. Soc., Dalton Trans.* **1992**, 427.
(16) King, C.; Khan, M. N. I.; Staples, R. J.; King, C.; Fackler, J. P., Jr. *Inorg. Chem.* **1992**, *31*, 3236.
(17) Khan, M. N. I.; Staples, R. J.; King, C.; Fackler, J. P., Jr.; Winpenny, R. E. P. *Inorg. Chem.* **1993**, *32*, 5800.
(18) Shie, S. J.; Li, D., Peng, S. M.; Che, C. M. *J. Chem. Soc., Dalton Trans.* **1993**, 195.
(19) Yam, V. W. W.; Lee. W. K. *J. Chem. Soc., Dalton Trans.* **1993**, 2097.
(20) Uang, R. H.; Chang, C. K.; Peng, S. M.; Che, C. M. *J. Chem. Soc., Chem. Commun.* **1994**, 2561.
(21) Forward, J. M.; Assefa, Z.; Fackler, J. P., Jr. *J. Am. Chem. Soc.* **1995**, *117*, 9103.
(22) Leung, K. H.; Phillips, D. L.; Mao, Z.; Che, C. M.; Miskowsky, V. M.; Chan, C. K. *Inorg. Chem.* **2002**, *41*, 2055.

(23) (a) Crespo, O.; Gimeno, M. C.; Laguna, A.; Jones, P. G. *J. Chem. Soc., Dalton Trans.* **1992**, 1601. (b) Crespo, O.; Gimeno, M. C.; Jones, P. G.; Laguna, A. *Inorg. Chem.* **1996**, *35*, 1361. (c) Crespo, O.; Gimeno, M. C.; Jones, P. G.; Laguna, A. *J. Chem Soc., Dalton Trans.* **1996**, 4583.
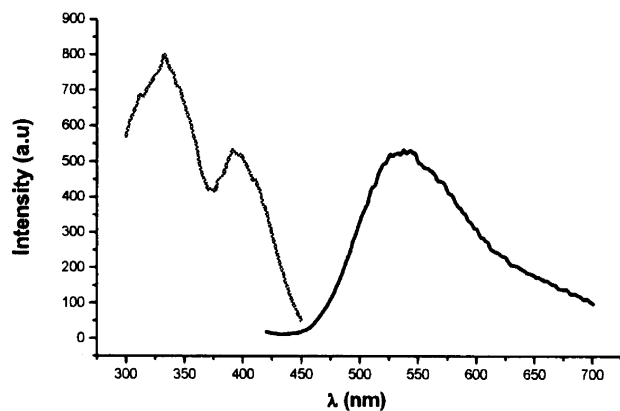
Figure 2. Emission and excitation spectra for the high energy emission in compound **7** in the solid state, at room temperature.

Figure 3. Emission and excitation spectra for **12** in the solid state, at room temperature.

important role in these radiative transitions. Moreover, the phenyl rings of the diphenyl-*nido*-diphosphine are not expected to be responsible for these excited states since the phenyl groups have their $^3(\pi\pi^*)$ state at higher energies. Thus, we propose that the transitions are more likely to be associated with the orbitals of the carborane cage.

Three-Coordinated Complexes. The absorption spectra of *nido*-carborane−diphosphine complexes and ligands display a common feature, a very intense band located at 310 nm ($\epsilon = 6500−1200$ M^{-1} cm^{-1}). Similar wavelengths have been reported for phenyl $^3(\pi\pi^*)$ intraligand (IL) transitions.[24] This is the origin we propose, although a definite assignment of this band is not possible since the electronic absorption spectra are fairly featureless. The only example without these groups, the diisopropyldiphosphine ligand (**2B**), does not show this band. Thus, an origin from the carborane cage is unlikely. Other possibilities, such as the assignation to a spin-allowed $(d\sigma^*)(p\sigma)$ transition, are also unlikely; such transitions have been described[14−16,19] for bands at higher energies.

In a manner similar to the free ligands (**1**, **2**), only the gold complexes containing *nido*-diphosphines are luminescent. The luminescence spectra of the diphenyl-*nido*-diphosphine derivatives display a high energy and a low energy emission in the solid state both at room temperature and at 77 K and in solution, while in the diisopropyl-*nido*-diphosphine analogues, only the high energy emission appears (see Table 1). These high and low energy emissions are different (in energy, shape, or both) from those in the free ligands and are related to the presence of gold and the monophosphines. The contribution of the metal center in each type of emission seems to occur in different ways. We have tentatively assigned these emissions to a metal-perturbed intraligand transition (a) and from a mainly metal-to-ligand charge transfer (MLCT) transition (b).

(a) Metal-Perturbed IL Transition. Regarding the high energy band, all the *nido*-complexes analyzed show a strong luminescence in the solid state at room temperature and at 77 K (Figures 2 and 3) and in solution. The spectra show a common excitation pattern with maxima located at about 330
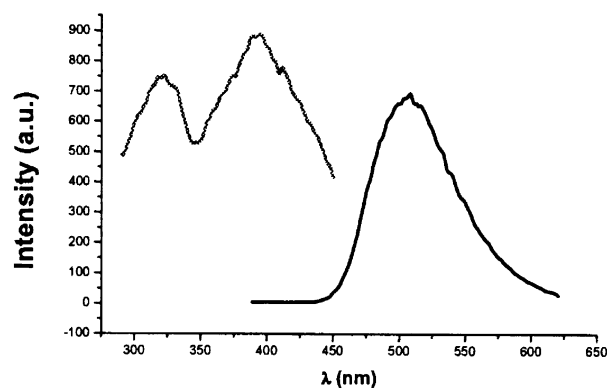
nm, in the solid state. The emissions (solid state) are located at about 510 nm (see Table 1: PR$_2$ = PPh$_2$, 513−540 at room temperature, 506−529 nm at 77 K; PR$_2$ = P^{i}Pr$_2$, 508−512 nm at room temperature, 503−507 nm at 77 K).

Comparison of these data with those obtained for the free ligands in the solid state shows similar excitation profiles (332 nm for diphenyl; 335 nm for the diisopropyl), although the corresponding emissions are shifted to higher energies compared with those of the gold complexes in both cases (482 nm for the diphenyl-*nido*-diphosphine (**2A**) and 484 nm for the diisopropyl-*nido*-diphosphine (**2B**)). Because of the similarity between data for complexes and ligands, we propose that these high energy transitions are likely to be primarily carborane cage intraligand (IL) in character, as has been suggested for the free ligands. However, this transition seems to be perturbed by a metal-centered (MC) contribution and/or by the contribution of the phosphorus substituents, which appears theoretically in the calculations (see later). Different emission energies are observed in each series when only the substituent at the diphosphine or only the mono-phosphine is modified. We postulate only an insignificant contribution to the excited state from the substituents at the phosphorus centers of the diphosphine, since they appear not to contribute in the free ligands (see preceding discussion). Thus, these differences probably come from the contribution to the excited state from the monophosphines bonded to gold, either directly or through the interaction with the gold center (MLCT), which perturbs the mainly intraligand excited state, giving rise to an admixture of IL and MLCT character. The emissions in these complexes are also temperature-dependent; in all cases, the emissions are blue-shifted at 77 K as compared to those at room temperature in the solid state (see Table 1). The blue shift of an emission band with decrease of temperature has been described previously and explained as a substantial dependence of the emission maxima on the environmental rigidity (luminescence rigidochromism).[25] In this case, the rigidity is likely to be associated predominantly with the carborane cages.

(b) MLCT Transition. Complexes **7**, **8**, and **9** show a low energy emission band at about 650 nm (see Table 1,

(24) (a) Tang, S. S.; Chang, C. P.; Lin, I. J. B.; Liou, L. S.; Wang, J. C. *Inorg. Chem.* **1997**, *36*, 2294. (b) Fernández, E. J.; Gimeno, M. C.; Laguna, A.; López de Luzuriaga, J. M.; Monge, M.; Pyykkö, P.; Sundholm, D. *J. Am. Chem. Soc.* **2000**, *122*, 7287.

(25) (a) Wang, S.; Garzón, G.; King, C.; Wang, J. C.; Fackler, J. P., Jr. *Inorg. Chem.* **1989**, *28*, 4623. (b) Lees, A. J. *Chem. Rev.* **1987**, *87*, 711.
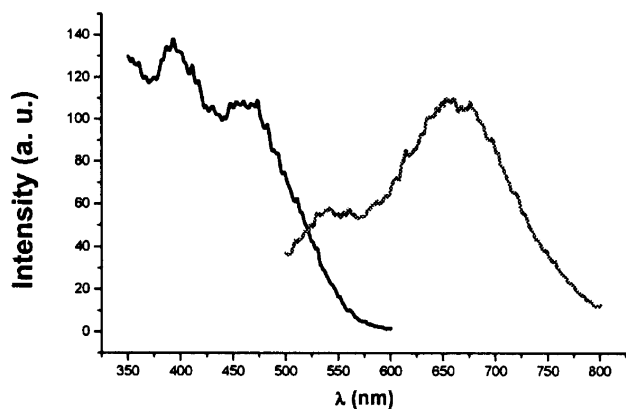
Figure 4. Emission and excitation spectra for the low energy emission in compound **7** in the solid state, at room temperature.

Figure 5. Crystal structure of compound **10**, radii are arbitrary. Hydrogen atoms have been omitted for clarity.

Figure 4) in the solid state, at room temperature and at 77 K, and in solution. This indicates the presence of a second emitting fluorophore. In the case of the isopropyl derivatives (**10**, **11**, **12**), only a certain degree of asymmetry in their emission bands could be detected, which could perhaps indicate an overlapping of both emissions.

In contrast to the previously discussed higher energy bands, a predominantly carborane character in the lower energy excited states is unlikely, since the emission energies are considerably shifted to the red (about 100 nm) compared to the free ligands. In this case, the assignment of these new bands observed in complexes **7**, **8**, and **9** is likely to be related to the three-coordination around the gold(I) center. The luminescence that arises from a three-coordinate gold(I) (D_{3h} symmetry) center is a general phenomenon where the origin of the emission has been assigned to a metal-centered transition $a(p_z) \rightarrow e(d_{x^2-y^2}, d_{xy})$, although there may be a mixing of some ligand character into the orbital manifold. A previous study of complexes $[Au(PR_3)_3]^+$ ($PR_3 = P^nBu_3$ and PPh_3) did not show dependence of the optical behavior on the phosphine.[16] In the case of our complexes, the emission is strongly dependent on the substituents at phosphorus, and thus, a more pronounced gold−phosphorus character is suggested, reinforcing the previous assignment. In this context, Che and co-workers[20] reported a different assignment for the visible emission in the dinuclear complex with two trigonal-planar P_3Au centers $[Au_2KL_3][ClO_4]_3 \cdot CH_2$-$Cl_2 \cdot 2MeOH \cdot 0.5H_2O$. The emission for this complex was assigned to an MLCT (metal to ligand charge transfer) [Au $\rightarrow \pi^*(L)$] excited state.[20] This assignment is in good agreement with our results because the charge transfer transition should be influenced by the donor/acceptor abilities of the phosphorus donor atoms bonded to gold. Accordingly, a decrease of the acceptor properties of the substituents at phosphorus centers should shift the emission bands to higher energies.

Complexes **7**, **8**, and **9**, in the solid state at room temperature, gave emissions at 670, 640, and 614 nm, which shifted to 676, 653, and 633 nm, respectively, at 77 K (see Table 1). Thus, the emission energies in the solid state, which follow the order **9** > **8** > **7**, may be indicative of an excited state bearing a large MLCT character for each complex, following an order in accordance with the π-acceptor ability
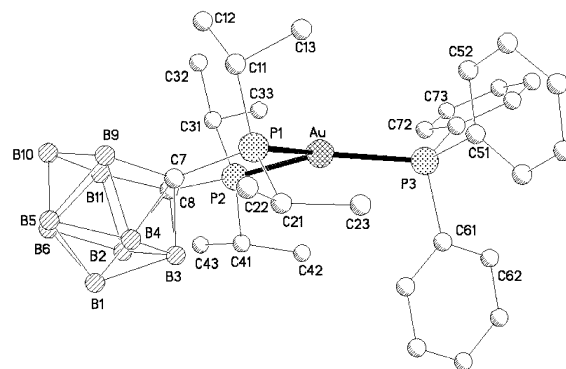
of the phosphines bonded to gold, $PPh_3 > PPh_2Me > P(4-MeC_6H_4)_3$.[26] The emissions are in the range reported by Che,[20] supporting their origin from a similar excited state. In contrast to the high energy bands that were assigned to be carborane-localized (see preceding discussion), in this case we observe a red shift in the emissions when the temperature is lowered at 77 K. The shift to lower energies with a decrease of temperature is a standard phenomenon in luminescent gold complexes and has been related to a thermal contraction of the bonds that leads to a reduction in the band gap energy.[10]

The absence of low energy emissions in the case of the diisopropyl derivatives **10**, **11**, and **12** is perhaps related to an overlap with the bands arising from the intraligand metal-perturbed excited state (high energy transitions). The shifts of these MLCT transitions to higher energies, if compared with the diphenylphosphine derivatives, are probably attributable to the diminished π-acceptor ability of the diisopropyl groups, or a significant contribution of a phosphorus (diphosphine) intraligand transition to the excited state.

Therefore, the low energy emissions may reasonably be assigned as arising from an admixture of IL and a mainly MLCT excited state, to whose character, obviously, the substituents at both types of phosphorus atoms contribute.

An alternative assignment, derived from a difference in the environment of gold(I) and/or an exciplex emission, would also lead to such findings. The similar behavior found in rigid media (suppressing exciplex formation) and in solution, and the ^{31}P NMR spectra, which are in accordance with the three-coordination (suppressing significant environment perturbation), agree with our proposals.

In short, these results extend Che's initial proposal for gold(I)−gold(I) interactions in the sense that, also in the case of three-coordinate gold(I) complexes, the role of the environment of gold(I) cannot be excluded and that gold−ligand bonding affects the photoluminescence of gold complexes.

Crystal Structure of $[Au\{(P^iPr_2)_2C_2B_9H_{10}\}(PPh_3)]$ (10). The crystal structure of $[Au\{(P^iPr_2)_2C_2B_9H_{10}\}(PPh_3)]$ (**10**) has been determined by X-ray diffraction studies (Figure 5). Comparison can be made with the previously reported [Au-

(26) Cotton, F. A.; Wilkinson, G.; Murillo, C.; Bochmann, M. In *Advanced Inorganic Chemistry*, 6th ed.; Wiley: New York, 1999; p 643.

Table 2. Comparison of Some Distances (Å) and Angles (deg) in Similar Complexes

compd	P(1)−Au−P(2)	Au−plane[b]	Au−P[c]	Au−P[d]	P−C	B−H[e]
[Au(dppcc)(PPh₃)]ClO₄[a]	90.2(1)	0.18	2.405(1)	2.318(1)	1.883(5)	
			2.417(1)		1.870(5)	
[Au(dppnc)(PPh₃)][a] **7**	84.91(4)	0.076	2.389(613)	2.2831(13)	1.827(5)	1.09
			2.3952(12)		1.832(5)	1.66
[Au(dipnc)(PPh₃)][a] **10**	90.38(2)	0.152	2.4083(6)	2.3791(6)	1.856(2)	1.08
			2.3076(6)		1.853(2)	1.41

[a] dppnc = (PPh₂)₂C₂B₁₀H₁₀, dppnc = [(PPh₂)C₂B₉H₁₀]⁻, dipnc = [(P^iPr₂)₂C₂B₉H₁₀]⁻. [b] Distance of gold from the plane formed by the three phosphorus atoms. [c] Au−P(diphosphine). [d] Au−P(monophosphine). [e] B−H distances to the bridging H atom of the open face.
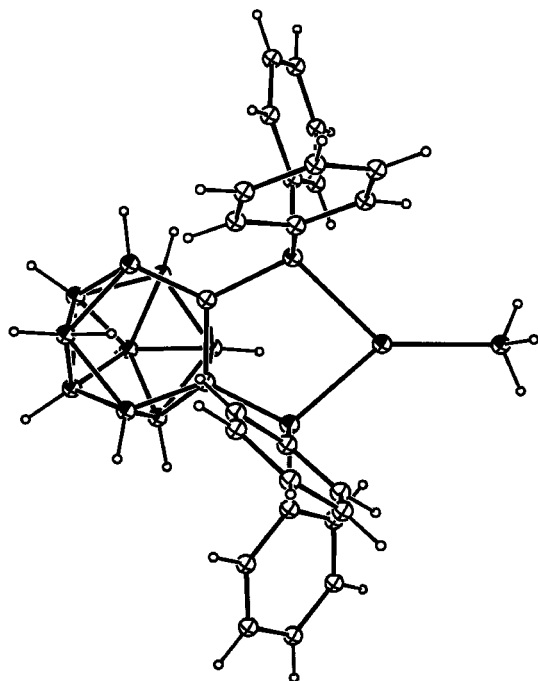
Figure 6. Theoretical model system for [Au{(PPh₂)₂C₂B₉H₁₀}(PH₃)].

{(PPh₂)₂C₂B₁₀H₁₀}(PH₃)]ClO₄[23a] and [Au{(PPh₂)₂C₂B₉H₁₀}-(PPh₃)][23b] (**7**) (Table 2). In [Au{(PPh₂)₂C₂B₁₀H₁₀}(PH₃)]ClO₄ and **10**, the gold atom lies somewhat out of the plane formed by the three phosphorus atoms. The major deviation from the ideal trigonal geometry is in all the cases represented by the restricted "bite" angle of the diphosphine (P(1)−Au−P(2)), which is found to be near 90° except for compound **7** (84.91(4)°). As is generally observed for complexes of the *nido*-ligand,[23c] the central boron atom B10 is of the C₂B₃ open face. In **10**, it is bonded to two hydrogen atoms, one of which is semibridging to the neighboring B11; the longest B−B bond is the bridged B10−B11 (1.851(4) Å, cf. B9−B10 1.813(4) Å).

DFT and TD-DFT Results. The interesting luminescence behavior experimentally observed for these three-coordinated gold(I) diphosphino−carboranes prompted us to study in detail the transitions responsible for it in one selected example. First, we performed single-point DFT calculations with a representative model system [Au{(PPh₂)₂C₂B₉H₁₀}-(PH₃)] (Figure 6) which was built from the X-ray diffraction results of complex [Au{(PPh₂)₂C₂B₉H₁₀}(PPh₃)] (**7**) using H atoms instead of phenyl rings in the monophosphine ligand in order to reduce the computational costs. Thus, we performed a population analysis based on the SCF orbitals to check the contribution of each atom of the molecule to

Table 3. Population Analysis for [Au{(PPh₂)₂C₂B₉H₁₀}(PH₃)] Model System: Contribution from Each Type of Atom to Occupied Orbitals HOMO and HOMO − 1

MO	% C₂B₉H₁₀	% Au	% PPh₂	% PH₃
HOMO (149ag)	56.4	9.2	32.7	1.6
HOMO − 1 (148ag)	45.1	11.8	41.3	1.8

the high energy occupied molecular orbitals 149a (HOMO) and 148a (HOMO − 1) (Figure 7), because these are the ones involved in the most intense theoretical excitations (see following discussion).

The results are given in Table 3, and the analysis of these data shows that in both orbitals (149a and 148a) the main contribution arises from the carborane cage (56.4% and 45.1%, respectively), although PPh₂ groups (32.7% and 41.3%) and the gold(I) center (9.2% and 11.8%) also contribute.

As regards virtual orbitals, they cannot be analyzed by a population analysis, but we can check their shape (Figure 7). The lowest unoccupied orbitals from LUMO + 1 to LUMO + 6 (involved in the theoretical excitations, see later) are localized mainly on the PPh₂ groups with an apparently small contribution from the carborane cage in the low energy empty orbitals 151a (LUMO + 1) and 152a (LUMO + 2) and from the gold center in the high energy orbitals 153a (LUMO + 3), 154a (LUMO + 4), and 156a (LUMO + 6). Thus, from single-point DFT calculations, it can be deduced that both the highest occupied and the lowest unoccupied orbitals are mainly based on the carborane ligand with some contribution from the gold(I) center, in agreement with the previously described experimental results which show that when gold(I) is present in the molecule, the arrival orbitals from which the emissions are produced have also a certain character from the gold and alkyl or aryl substituents on the carborane ligand. Going further, we have confirmed the participation of the commented orbitals in the photoluminescence properties. Thus, the first few allowed excitation energies of the [Au{(PPh₂)₂C₂B₉H₁₀}(PH₃)] model system were calculated at the time-dependent-density functional theory level (TD-DFT) as described in the computational details found in the Experimental Section. In them, we cannot at present estimate the strength given by spin−orbit effects to the forbidden transitions. Therefore, only allowed transitions were considered in these quasirelativistic calculations.

In Figure 8, we show the calculated excitations A−J compared with the experimental excitation spectrum of complex **7** in the solid state. The predicted energy values for the excitations clearly match the experimental excitation spectra. Moreover, both in the experimental and in the
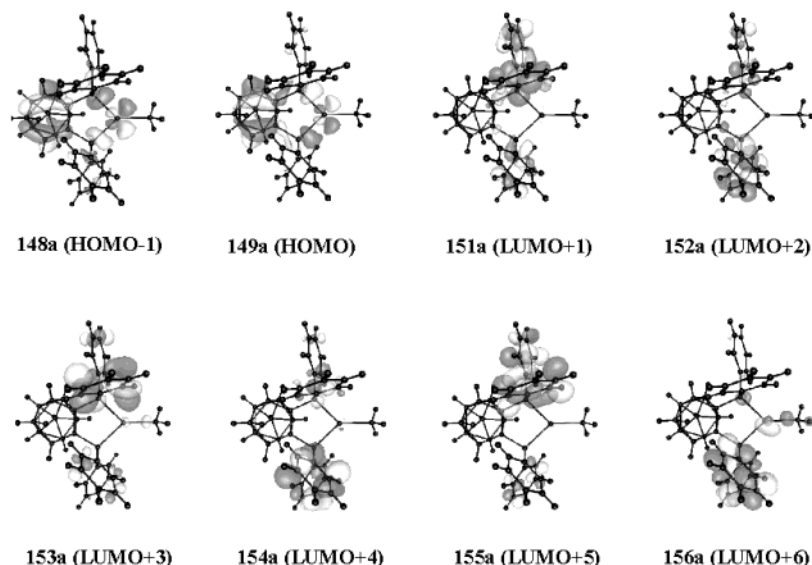
Figure 7. Molecular orbitals HOMO, HOMO − 1, and those from LUMO + 1 to LUMO + 6, involved in the theoretical calculations.
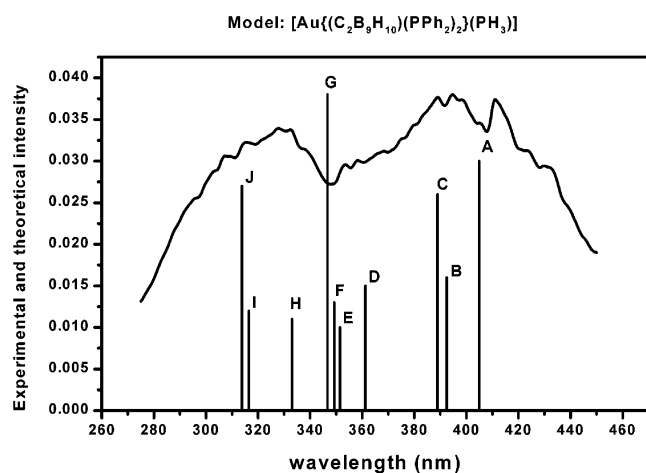

Figure 8. Experimental excitation spectra for complex [Au{(PPh$_2$)$_2$C$_2$B$_9$H$_{10}$}-(PPh$_3$)] (**7**) in the solid state and theoretical oscillator strengths, f, from Table 4 for the model [Au{(PPh$_2$)$_2$C$_2$B$_9$H$_{10}$}(PH$_3$)].

Table 4. TD-DFT RPA Allowed Excitation Calculations for [Au{(PPh$_2$)$_2$C$_2$B$_9$H$_{10}$}(PH$_3$)]

excitation	λ_{calcd} (nm)	λ_{exptl} (nm)	oscil str (s)[a]	contribution[b]
A	404.9		0.310×10^{-1}	149a ⟶ 151a
B	392.5	394.5	0.160×10^{-1}	149a ⟶ 152a (73.3)
				149a ⟶ 153a (23.0)
C	388.9		0.260×10^{-1}	149a ⟶ 153a (69.0)
				149a ⟶ 152a (22.3)
D	361.2		0.150×10^{-1}	148a ⟶ 151a
E	351.5		0.100×10^{-1}	149a ⟶ 155a (80.0)
				148a ⟶ 153a (14.0)
F	349.3		0.130×10^{-1}	149a ⟶ 156a (54.6)
				148a ⟶ 152a (25.4)
				148a ⟶ 153a (14.0)
G	346.7		0.380×10^{-1}	148a ⟶ 153a (69.0)
				149a ⟶ 155a (11.0)
H	333.1	330.0	0.110×10^{-1}	148a ⟶ 154a (89.4)
				149a ⟶ 158a (5.3)
I	316.5		0.120×10^{-1}	148a ⟶ 155a
J	313.9		0.270×10^{-1}	148a ⟶ 156a

[a] Oscillator strength shows the mixed representation of both velocity and length representations. [b] Value is $|coeff|^2 \times 100$.

theoretical spectra two equivalent groups of signals can be observed (from A to C and from D to J) that display relative energy differences between them with good agreement between theory and experiment.

Finally, the analysis of the orbitals involved in each transition (Table 4) shows that all the excitations come from orbitals HOMO (149a) and HOMO − 1 (148a), which are mainly located at the carborane cage with a contribution from the PPh$_2$ groups and the gold(I) center, and reach the diphenyl−phosphino-based orbitals with some influence of the carborane cage (LUMO + 1 and LUMO + 2) and the gold(I) center (from LUMO + 3 to LUMO + 6). These predicted excitations are in agreement with the experimental data observed for the high energy excitation and emission bands of the *nido*-phosphino−carborane gold(I) complexes. The low energy excitation and emission bands experimentally observed for the diphenylphosphino−carborane derivatives have not been reproduced by the TD-DFT approach. This fact could be associated with a possible forbidden character of this low energy transition assigned as an MLCT (metal

to ligand(diphosphine)−ligand(monophosphine) charge transfer). As we have already commented, only allowed transitions have been analyzed.

Experimental Section

Instrumentation. The C and H analyses were carried out with a Perkin-Elmer 2400 microanalyzer. Mass spectra were recorded on a VG Autospec, with the (liquid secondary ion mass spectra) LSIMS technique, using nitrobenzyl alcohol as matrix. NMR spectra were recorded on a Varian Unity 300 spectrometer and a Bruker ARX 300 spectrometer in CDCl$_3$. Chemical shifts are cited relative to SiMe$_4$ (^{1}H, external), and 85% H$_3$PO$_4$ (^{31}P, external).

Synthesis. The starting materials [AuCl(PR$_3$)],[27] [1,2-(PPh$_2$)$_2$C$_2$B$_{10}$H$_{10}$],[12] and [1,2-(P^{i}Pr$_2$)$_2$C$_2$B$_{10}$H$_{10}$][29] were prepared according to published methods. Complexes **1**−**6** were synthesized as described[23a] for the analogous perchlorate salts of [1,2-(PPh$_2$)$_2$C$_2$B$_{10}$H$_{10}$], using [Au(OTf)L] as starting material, prepared

(27) Usón, R.; Laguna, A. *Inorg. Synth.* **1980**, *21*, 71.
(28) Alexander, R. P.; Schroeder, H. *Inorg. Chem.* **1963**, *2*, 1107.
(29) Teixidor, F.; Viñas, C.; Abad, M. M.; Núñez, R.; Kivekäs, R.; Sillanpää, R. *J. Organomet. Chem.* **1995**, *503*, 193.

Table 5.

complex	yield (%)	anal. %C	data %H	%S	mass spectra [M]^a (%)^b	NMR data/J (Hz)
1	94	48.5	4.25	3.3	972 (100)	¹H: 1.30−3.30 (m, br, 10H, BH), 7.3−7.9 (m, 35H, Ph)
		(48.2)	(4.0)	(2.85)		³¹P{¹H}: (AB₂), δA = 44.8, δB = 60.4, J_{AB} = 136.3 Hz
2	95	45.50	4.4	3.55	911 (79)	¹H: 1.30−3.30 (m, br, 10H, BH), 2.45 (d, 3H, CH₃, J_{PH} = 9.2 Hz), 7.4−7.8 (m, 30H, Ph)
		(45.35)	(4.10)	(3.05)		³¹P{¹H}: (AB₂), δA = 27.0, δB = 59.5, J_{AB} = 138.8 Hz
3	89	47.85	4.2	2.95	1062 (100)	¹H: 1.30−3.30 (m, br, 10H, BH), 3.8 (s, 9H, OCH₃), 6.8−7.8 (m, 32H, Ph)
		(47.6)	(4.25)	(2.76)		³¹P{¹H}: (AB₂), δA = 41.1, δB = 60.0, J_{AB} = 139.0 Hz
4	89	40.4	5.65	3.75	837 (57)	¹H: 1−3 (m, br, 10H, BH), 1.28 (m, br, 24H, ^{i}Pr−CH₃), 2.73 (m, br, 4H, ^{i}Pr-CH), 7.4−8.2 (m, br, 15H, Ph)
		(40.25)	(5.4)	(3.25)		³¹P{¹H}: 43.5 (t, 1P), 87.2 (d, 2P), J_{PP} = 136.2 Hz
5	72	30.6	5.75	3.8	774 (100)	¹H: 1−3 (m, br, 10H, BH), 1.30 (m, br, 24H, ^{i}Pr-CH₃), 2.43 (d, 3H, CH₃, J_{PH} = 9.1 Hz), 2.79 (m, br, 4H, ^{i}Pr-CH), 7.5−8.4 (m, br, 10H, Ph)
		(30.75)	(5.55)	(3.45)		³¹P{¹H}: 25.5 (t, 1P), 89.4 (d, 2P), J_{PP} = 137.1 Hz
6	58	40.35	5.8	3.1	926 (100)	¹H: 1−3 (m, br, 10H, BH), 1.30 (m, br, 24H, ^{i}Pr−CH₃), 2.75 (m, br, 4H, ^{i}Pr-CH), 3.89 (s, 9H, OCH₃), 6.8−7.4 (m, br, 12H, Ph)
		(40.2)	(5.53)	(3.0)		³¹P{¹H}: 40.3 (t, 1P), 87.1 (d, 2P), J_{PP} = 138.0 Hz
10	70	46.8	6.75		824 (57)	¹H: −2.75 (m, br, 1H, BHB), 1−3 (m, br, 9H, BH), 1.28 (m, br, 24H, ^{i}Pr-CH₃), 2.73 (m, br, 4H, ^{i}Pr-CH), 7.3−7.6 (m, br, 15H, Ph)
		(46.6)	(6.5)			³¹P{¹H}: 45.4 (t, 1P), 85.5 (d, 2P), J_{PP} = 129.0 Hz
11	74	42.75	7.15		762 (36)	¹H: −2.8 (m, br, 1H, BHB), 1−3 (m, br, 9H, BH), 0.99 (m, br, 12H, ^{i}Pr-CH₃), 1.30 (m, br, 12H, ^{i}Pr-CH₃), 2.07 (m, br, 2H, ^{i}Pr-CH), 2.78 (m, br, 2H, ^{i}Pr-CH), 2.14 (d, 3H, CH₃, J_{PH} = 8.24 Hz), 7.4−7.6 (m, br, 10H, Ph)
		(42.5)	(6.75)			³¹P{¹H}: 25.8 (t, 1P), 88.8 (d, 2P), J_{PP} = 130.4 Hz
12	63	45.7	6.45		914 (21)	¹H: −2.8 (m, br, 1H, BHB), 1−3 (m, br, 9H, BH), 1.16 (m, br, 24H, ^{i}Pr-CH₃), 2.24−2.8 (m, br, 4H, ^{i}Pr-CH), 3.82 (s, 9H, OCH₃), 6.8−7.4 (m, br, 12H, Ph)
		(45.95)	(6.5)			³¹P{¹H}: 41.8 (t, 1P), 85.5 (d, 2P), J_{PP} = 131.1 Hz

^{a} Molecular (*nido*-species) or cationic molecular peak (*closo*-species). ^{b} Intensity of the peak.

by reaction of AgOTf with [AuClL]. Complexes **10−12** were prepared as described[23b] for compounds **7−9**. Table 5 shows the data for the new complexes.

Luminescence Measurements. Luminescence measurements were carried out using a Perkin-Elmer LS-50B luminescence spectrometer. Emission and excitation spectra were not corrected for instrumental response. Solid-state samples were packed into capillary tubes and introduced into the Perkin-Elmer variable-temperature accessory. Slit widths for excitation and emission monochromators were set at 4 nm.

Absorption Measurements. Electronic absorption spectra were obtained on a Shimadzu UV-2401 PC UV−vis recording spectrophotometer with 5×10^{-4} M acetone solutions. Acetone for photophysics was distilled over potassium permanganate and degassed before use.

Crystal Data for Compound 10. $C_{64}H_{110}Au_2B_{18}P_6$, M_r = 1653.85, orthorhombic, space group *Pbca*, a = 17.7478(16) Å, b = 19.8792(18) Å, c = 21.3960(18) Å, U = 7548.8(12) Å³, Z = 4, D_c = 1.455 Mg m⁻³, λ(Mo Kα) = 0.07173, μ = 4.047 mm⁻¹, $F(000)$ = 3328, T = −130 °C, yellow prism 0.36 × 0.16 × 0.12 mm³. The 125800 intensities were recorded to $2\theta_{max}$ 60° (BRUKER Smart 1000-CCD diffractometer), of which 11032 were unique (R_{int} = 0.0663) after absorption corrections using SADABS. The structure was solved by the heavy-atom method and subjected to full-matrix least-squares refinement on F^2 (program SHELXL-97).[30] All non-hydrogen atoms were refined anisotropically. H atoms were included using a riding model, except for those of the carborane open face, which were refined freely (although restrained with SADI). Refinement proceeded to wR(F^2) = 0.0521, conventional

$R(F)$ = 0.0232 for 422 parameters and 193 restraints (to light atom U values and local ring geometry), $S(F^2)$ = 0.976; maximum $\Delta\rho$ = 1.49 e Å⁻³.

Computational Methods. The molecular structure used in the theoretical studies of [Au{(PPh₂)₂C₂B₉H₁₀}(PH₃)] (Figure 8) was taken from the X-ray diffraction results for [Au{(PPh₂)₂C₂B₉H₁₀}-(PPh₃)] (**7**). Keeping all distances, angles, and dihedral angles frozen, single-point DFT calculations were performed on the model. In both the single-point ground-state calculations and the subsequent calculations of the electronic excitation spectra, the default Beck−Perdew (B−P) functional,[31−33] as implemented in TURBOMOLE,[34] was employed. The excitation energies were obtained at the density functional level using the time-dependent perturbation theory approach (TD-DFT)[34−39] which is a density functional theory generalization of the Hartree−Fock linear response (HF-LR) or random phase approximation (RPA) method.[40] In all calculations, the Karlsruhe split-valence quality basis sets[41] augmented with polarization functions[42] were employed (SVP). The Stuttgart

(30) Sheldrick, G. M. *SHELXL-97. A program for Crystal Structure Refinement*; University of Göttingen: Göttingen, Germany 1997.

(31) Vosko, S. H.; Wilk, L.; Nusair, M. *Can. J. Phys.* **1980**, *58*, 1200.
(32) Perdew, J. P. *Phys. Rev. B* **1986**, *33*, 8822.
(33) Becke, A. D. *Phys. Rev. B* **1988**, *38*, 3098.
(34) Ahlrichs, R.; Bär, M.; Häser, M.; Horn, H.; Köhmel, C. *Chem. Phys. Lett.* **1989**, *162*, 165.
(35) Bauernschmitt, R.; Ahlrichs, R. *Chem. Phys. Lett.* **1996**, *256*, 454.
(36) Bauernschmitt, R.; Ahlrichs, R. *J. Chem. Phys.* **1996**, *104*, 9047.
(37) Bauernschmitt, R.; Häser, M.; Treutler, O.; Ahlrichs, R. *Chem. Phys. Lett.* **1997**, *264*, 573 and references therein.
(38) Gross, E. K. U.; Kohn, W. *Adv. Quantum Chem.* **1990**, *21*, 255.
(39) Casida, M. E. In *Recent advances in density functional methods*; Chong, D. P., Ed.; World Scientific: River Edge, NJ, 1995; Vol 1.
(40) Olsen, J.; Jørgensen, P. In *Modern Electronic Structure Theory*; Yarkony, D. R., Ed.; World Scientific: River Edge, NJ, 1995; Vol. 2.
(41) Schäfer, A.; Horn, H.; Ahlrichs, R. *J. Chem. Phys.* **1992**, *97*, 2571.
(42) Dunning, T. H., Jr. *J. Chem. Phys.* **1994**, *100*, 5829.

effective core potentials implemented in TURBOMOLE were used for Au.[43] Calculations were performed without assuming any symmetry for the model.

Supporting Information Available: X-ray crystallographic file, in CIF format, for compound **10** . This material is available free of charge via the Internet at http://pubs.acs.org.

IC0259843

(43) Andrae, D.; Haeussermann, U.; Dolg, M.; Stoll, H.; Preuss, H. *Theor. Chim. Acta.* **1990**, *77*, 123.